Analytical Methods

Accepted Manuscript

Chiral Recognition of Naproxen Enantiomers Using Starch Capped Silver Nanoparticles

Javad Tashkhourian[*], Mina Afsharinejad

Department of Chemistry, Faculty of Sciences, Shiraz University, Shiraz, 71454, Iran

*Corresponding author:

Department of Chemistry, College of Sciences, Shiraz University, Shiraz, Iran

E-mail address: tashkhourian@susc.ac.ir (J. Tashkhourian)

1

Abstract

A novel, simple and inexpensive method for determination of naproxen enantiomers has been presented based on starch-capped Ag nanoparticles using spectrophotometric technique. Morphology and structure of the starch-capped Ag nanoparticles were characterized by transmission electron microscopy, X-ray diffraction and infrared spectroscopy. Under optimum experimental conditions, it was revealed that starch as a chiral selector could enantioselectively recognize naproxen enantiomers. Naproxen enantiomers were determined over a concentration range of 3.2×10^{-6} -1.4×10^{-4} M with a detection limit of 2.7×10^{-6} M. The results showed a relative standard deviation of 1.0 % and a relative error of -5.6 % for analysis of naproxen enantiomers in real samples.

Introduction

One distinctive biochemical signature of life is the high selectivity of chiral molecule species. With the dramatic increase in the use of chiral drugs, since the body exhibits different physiological responses to different enantiomers, chiral recognition has become a research focus in chemical, biological, and pharmaceutical sciences [1]. Research on enantiomeric recognition of chiral compounds can provide important information to understand the recognition process in biological systems. Although some progress in chiral discrimination has been achieved during the past decades [2], the selective detection of an individual enantiomer is still the most difficult analytical task owing to the similar physical and chemical properties as well as the similar molecular configurations of chiral isomers. Therefore, it is important to develop practical and rapid available methods for the chiral recognition of enantiomers [3]. Over the past decades, many methods for distinguishing chiral molecules have been reported, such as high-performance liquid chromatography [4], gas chromatography [5], capillary electrophoresis [6] etc. But most of them are time-consuming and impractical for a real time, multiplex, or high-throughput format. Therefore, it is still highly desirable to develop a simple, rapid, sensitive, and high throughput routine assay for chiral recognition. In particular, solution-based sensor systems capable of chiral recognition are of tremendous pharmaceutical value [7]. The key step in chiral analysis is formation of diastereoisomer complexes between a chiral selector and enantiomers [8]. A chiral selector must be a pure enantiomer which provides significant interactions (such as dispersive, π-π, n-π, and hydrogen bonding, ion-ion and ion-dipole interactions) at least with three functional groups around the chirality center of one enantiomer and with two functional groups of the other [9-10]. Generally, both enantiomers have different interactions with the chiral selector but the presence of similar functionalities in the chiral selector may lead to competitive binding of analogue sites [11].

3

Metal nanoparticles have important applications in nanotechnology because of their physicochemical properties based on their small size and high surface area [12]. Especially, silver nanoparticles (AgNPs) have significant applications in various fields because of their unique optical [13], electronical [14], an-microbial [15], catalytical and thermal properties [16, 17]. The AgNPs are usually prepared by reducing $AgNO_3$ with sodium citrate and sodium borohydride, and the resulting nanoparticles are capped with the citrate group [18]. Moreover, some capping agents such as starch and β-D-glucose were utilized to stabilize AgNPs such as starch as a reducing agent [19]. Glucose is one of the most widely-used green reducing agent due to its chemical reaction rate which allows a compromise between the number of nuclei created and the rate of growth of the silver nanoparticles [20]. The extensive number of hydroxyl groups present in starch can facilitate the complexation of silver ions to the molecular matrix. Analogously, it is plausible that silver ions can play a significant role in guiding the supramolecular organization among starch molecules.

Naproxen 6-methoxy-a-2-naphtalene acetic acid is a non-steroidal anti-inflammatory drug that exhibits analgesic and antipyretic properties. It is used for treatment of fever, inflammation, rheumatoid arthritis, primary dysmenorrheal and gout [21]. The critical role of naproxen in human health emphasizes its determination in biological fluids and drug formulations. S-naproxen shows desirable therapeutic properties and is 28 times higher active than R-naproxen [22]. Therefore, determination of enantiomer composition of naproxen is the concern of the life science studies [23].

Herein, for the first time, a simple and reliable method for the quantitative determination of naproxen enantiomers in aqueous solution is presented. Starch -capped silver nanoparticles (AgNPs) without any prior derivatization and sample preparation, have been used was presented. Based on these features AgNPs capped with starch as chiral selector was used for determination of naproxen enantiomers.

4

Experimental

Reagents

R-naproxen and S-naproxen, starch, methanol and $AgNO_3$ were purchased from Merck. D-Glucose and potassium hydrogen phthalate (KHP) were purchased from Fluka. All other chemicals were analytical reagent grade and used directly without further purification. Distilled water was used throughout the experiments. To prepare 0.1 M of R and S-naproxen solutions, aliquot of 23.0 mg of each enantiomer was introduced into individual 5-mL volumetric flasks and was diluted to the mark by methanol. To prepare KHP buffer with pH values in the range of 3.6 -6.5, the NaOH solution was gradually added to a selected volume of KHP solution until the pH meter showed the desired pH value. For real sample analysis, five tablets of naproxen were accurately weighed and ground and its solution was prepared by dissolving 630.0 mg of the powder in methanol and filtering the solution. The prepared solution contained a specified amount of NAP (500 mg).

Apparatus

 The UV-Vis spectra were recorded using Unico 4802 UV-Vis double beam spectrophotometer employing quartz or glass cuvette with 1.0 cm path length. The temperature of the cell compartment was thermostated at $28 \pm 0.1°C$ by circulating water from a thermostated bath. The FT-IR spectroscopy (FTIR-8300 Shimadzu), attenuated total reflection (ATR) spectroscopy using Perkin-Elmer FT-IR spectrophotometer (model Spectrum RX I), circular dichroism spectroscopy measurements were done in a 0.1 cm path length cuvette, using an Aviv model 215 Spectropolarimeter (Lakewood, NJ, USA).   XRD (Bruker D8 Advance with Cu-Kα, λ=0.1542 nm) and the transmission electron microcopy (Zeiss –EM10C-80KV) were used for characterization of AgNPs. The pH measurements

were made with a Metrohm 780 pH meter using a combined glass electrode. The synthesized

AgNPs were separated by using a high speed centrifuge working at 20000 rpm.

Synthesis of starch-capped silver nanoparticles

Starch-capped silver nanoparticles were synthesized through a classical reduction method

[19].The method is based on the reduction of $AgNO_3$ by glucose in the presence of starch,

acting as both stabilizing and protecting agent. In particular, 0.4 g soluble starch (medium

molecular weight) was dissolved in 200.0 mL deionized water. Then 100.0 mL of this

solution was added to a mixture of 2.0 mL of 0.1 M $AgNO_3$ (0.1 M) and 5.0 mL of 0.1 M

glucose. The solution was heated and boils the solution for 30 minutes and turn into yellow.

The produced starch capped silver nanoparticles, which form a stable dispersion in water,

was kept at room temperature.

Calculation concentration of AgNPs

The concentration of the AgNPs solution was calculated using Beer's law [24] and extinction

coefficient (ε) of AgNPs (the extinction coefficient for the silver particles is calculated using

the following equation:

$$\ln \varepsilon = 1.4418 \ln D + 18.955$$

D is the diameter in nm from TEM image of AgNPs.

General procedure

Determination of naproxen enantiomers was performed at (28 °C). During experiments 200.0

μL of synthesized starch-AgNPs was diluted with 700.0 μL of KHP buffer (pH 6.0, 0.01 M).

Then 1.4×10^{-4} M R-and S-naproxen were added to this solution. The UV-Vis spectra were

obtained after 8 min.

6

Results and discussion

Characterization of silver nanoparticles

The prepared silver nanoparticles showed a plasmon resonance peak at 400 nm as shown in Fig. 1. This is a typical absorption band of spherical AgNPs due to their surface plasmon resonance band. The FT-IR spectra of both soluble starch and starch-capped AgNPs are shown in Fig 2, it has been reported [25] that in 3600–2800 cm^{-1} region, strong hydrogen-bonded (O–H) stretching absorptions and weak C–H stretching absorptions are usually observed. The starch-capped AgNPs spectrum had characteristic broad and strong absorbance bands at 3450 cm^{-1}, 1643 cm^{-1} and 2923 cm^{-1} which could be assigned to the hydroxyl (O-H) group and C-H stretching vibrations, respectively. A shift from 3450 cm^{-1} to 3417 cm^{-1} is observed for stabilized AgNPs; this may be due to the inter and intra molecular interactions of Ag^0 with –OH group [25]. The morphology of the resulting starch-AgNPs composite was characterized by TEM image as shown in Fig. 3. As it can be seen, AgNPs were monodispersed and were spherical in shape. The X-ray diffraction pattern was also carried out for the powder sample of starch-AgNPs. A typical diffraction pattern for AgNPs is shown in Fig. 4. The Bragg reflection peaks appeared at (111), (200), and (311) were indexed to the silver metal with face centered cubic structure.

Figure 1

Figure 2

Figure 3

Figure 4

Enantioselective recognition of naproxen enantiomers

Naproxen in methanol showed two peaks absorption at 262 and 273 nm as demonstrated for it solution of 1.4×10^{-4} M shown in Fig.5 (a). By adding naproxen enantiomers to starch-

capped AgNPs solution, no significant changes in plasmon resonance peak of silver nanoparticles at 400 nm was occurred. However, a significant shift to 312 and 323 nm was observed. The absorbance spectra were shown in Fig. 5 (b). As it is shown in this figure, there are significant differences between responses R and S naproxen enantiomers in these wavelengths. An aliquot of 200.0 μL of starch-capped AgNPs in of 0.01 M potassium hydrogen phthalate buffer, pH=6.0, was introduced into a 10-mm quartz cuvette, Then, 100.0 μL of (0.001 M) R or S -naproxen was added to the quartz cuvette. The differences between of the absorption peaks (ΔA) measured 7.0 min after addition of individual enantiomers is shown in Fig. 5 (b) and enantiomer in the presence of starch-capped AgNPs. The change in the absorption peak indicates that the interaction of S-NAP with the nanoparticles is more than R-NAP. For comparison individual, absorbance spectrum of naproxen enantiomers in KHP buffer and also starch were obtained, respectively. The results show that there is no significant change in the absorption peak of naproxen enantiomers in the absence of AgNPs. However, the slightly difference of adsorption peak of R and S-naproxen observed in starch solution that this might lead to the difference in the free energy of attachment of these enantiomers and starch which reflects as different in absorbance. Citrate-capped AgNPs and the bare AgNPs were synthesized through direct reaction of $AgNO_3$ aqueous solution and $NaBH_4$ aqueous solution. The responses of bare AgNPs, citrate-capped AgNPs and starch-capped AgNPs to R- and S-NAP were compared. The experimental results show that bare AgNPs and citrate-capped AgNPs could not discriminate R- and S-NAP, and only starch-capped AgNPs were equipped with the better ability of discrimination between R-and S-NAP.

According to Dalgliesh's theory [26], interactions in at least three configuration-dependent points are required for a chiral selector to recognize enantiomers [27]. Discrimination can be based on the thermodynamic enantioselectivity, and the difference in

8

the free energies.   The structure of aromatic ring of naproxen and the intermolecular

hydrogen bond between naproxen and starch could possibly provide this "three-point"

interaction. It was supposed that intermolecular hydrogen bond between naproxen and starch

and electrostatic interaction could possibly give this recognition.

Figure 5

 For further study the interaction of R- and S-NAP with starch-capped AgNPs were

investigated by circular dichroism spectroscopy and the results were shown in Fig. 6. The

spectra demonstrate that there are significant differences between responses R and S

enantiomers and the change in the peak indicates that the interaction of S-NAP with the

nanoparticles is more than R-NAP.

Figure 6

Effect of pH and ionic strength

The effects of different pH values on the adsorption process have been investigated in the pH

range of 3.0 to 8.0. In the pH <3.0 and pH > 8.0 the silver nanoparticles are not stable and

aggregate. So, the pH range of 3.5 to 8.0 adjusted by different buffers was investigated. Fig.

7a shows the effect of pH on the change of absorption peak for R and S-naproxen in KHP

buffer .As it is shown, the most suitable signal for differentiating the naproxen enantiomers

have been obtained in pH 6.0 adjusted by KHP buffer. Different concentrations of this buffer

were examined and the results are shown in Fig. 7b. The results show that the lower

concentration of the buffer is more suitable. This can be attributed to the effect of ionic

strength. When the ionic strength increases, the interaction of NAP enantiomers with AgNPs

and ΔA is reduced. This could be due to the interactions of ions with NAP enantiomers that

inhibit the interaction of NAP with AgNPs.

Figure 7

Optimization of AgNPs solution volume

The AgNPs concentration has an undeniable effect on the sensitivity and linearity of determination. Since absorption peaks for both S- and R-NAP were increased with increasing AgNPs concentration, , the volume of AgNPs was optimized. To do this, different amounts of AgNPs were prepared and used for studying the interaction with 100.0 μL of 0.001 M NAP enantiomers. The results are shown in Fig. 7c. Since high volume of AgNPs may cause deviation from Beer's law, and lower volume may lead to lower sensitivity. According to the equation size of discussed, the calculated concentration of starch-capped AgNPs with D = 24 nm and $\varepsilon = 10^{10}$ M^{-1} cm^{-1} was 8.0×10^{-11} M so 200.0 μL of this stock solution was used for further studies.

Effect of temperature

Fig. 7d shows the effect of temperature on the interaction of starch-capped AgNPs with naproxen enantiomers. The maximum differences of the absorption peak (ΔA) occurred at 28 $^{\circ}$C and were stable afterwards.

Optimization of incubation time

The effect of the reaction time on the differences of the absorption peak (ΔA) of starch-capped AgNPs with R and S-naproxen was investigated. As it is shown in Fig. 7e, the maximum difference in the absorption occurred after about 8.0 minute.

Calibration curve

As shown in Fig. 8 under the optimum condition, the absorption spectra of AgNPs were recorded in the presence of different amounts of NAP enantiomers. The calibration curve for NAP enantiomers was linear in the concentration range of 3.2×10^{-6} to 1.4×10^{-4} M with a correlation coefficient of 0.999 (Fig. 9). The limit of detection (LOD) was calculated using $3\sigma_b/k$ equation (σ_b is the standard deviation of blank and k is the slope of calibration curve). The LOD of the method was found to be 2.7×10^{-6} M. The differences of peak absorption (ΔA) were significant between S-and R-NAP at all concentrations.

Figure 8

Figure 9

Repeatability

In order to examine the repeatability of the developed method, five samples of 1.4×10^{-4} M of R- and S-NAP were prepared and tested under optimum condition and the absorption spectra were recorded. The relative standard deviation (RSD) for 5 measurements was 1.25% for S-NAP and 1.4% for R-NAP, which shows that the method possesses good repeatability for R- and S-NAP. Therefore, the method supposed to have a good repeatability for chiral determination of naproxen enantiomers.

Determination of synthetic samples analysis

The starch- AgNPs were applied to measure the absorption response of a series of solutions that were prepared by mixing S- and R-NAP at different fixed ratios as shown in Fig. 10. The difference of the relative absorption and the enantiomers ratio are shown in Fig. 11 indicating

that the enantiomeric composition of NAP can be resolved from the corresponding linear calibration curves.

Figure 10

Figure 11

Real samples analysis

The proposed method was developed to the determination of naproxen in commercially available naproxen tablets. Five tablets were accurately weighed and ground and its solution was prepared by dissolving 630.0 mg of the powder in methanol and filtering the solution. The prepared solution contained a specified amount of NAP (500 mg). Three samples with different enantiomeric composition of S-NAP, which were prepared by spiking enantiomer mixture to starch-capped AgNPs solution, were analyzed. The results are presented in Table 2 along with the corresponding precision and accuracy of the measurement. A mixture of the enantiomers with a total concentration of 1.4×10^{-4} M was also tested and a relative standard deviation (RSD) of 1.0 % was obtained.

Conclusion

Starch-capped AgNPs were found to be an appropriate probe for analysis of naproxen enantiomers by using UV-Vis spectrophotometry. The results showed that the measured signal was higher for S-naproxen when interacted with AgNPs under the same experimental conditions. The precision, accuracy, and linear dynamic range of developed method show that the figures of merit were comparable or better than most procedures reported for naproxen determination (Table 2) [28-31].

12

Analytical Methods Accepted Manuscript

Reference

[1] T.Q. Yan,C. Orihuel, Rapid and high throughput separation technologies: steady state recycling and supercritical fluid chromatography for chiral resolution of pharmaceutical intermediates J. Chromatogr. A. 1156 (2007) 220

[2] Y.Z. Fu, L.L. Wang, Q. Chen, J. Zhou, Enantioselective recognition of chiral mandelic acid in the presence of Zn(II) ions by l-cysteine-modified electrode Sens. Actuat. B 155 (2011) 140

[3] R. Natarajan, S.C. Basak, T.S. Neumann, Novel approach for the numerical characterization of molecular chirality. J. Chem. Inf. Model. 47 (2007) 771

[4] L.-M. Yuan, Effect of mobile phase additive on chiral separation Separation and Purification Technology 63 (2008) 701

[5] J. Din, T. Welton, D. W. Armstrong, Chiral Ionic Liquids as Stationary Phases in Gas Chromatography Anal. Chem.76 (2004),6819.

[6] M. Kato,T.Toyo Oka, Enantiomeric separation by CEC using chiral stationary pases, Chromatography,22,(2001) 159

[7] M.Zhang, B. C. Ye, Colorimetric Chiral Recognition of Enantiomers Using the Nucleotide-Capped Silver Nanoparticles Anal. Chem. 83 (2011) 1504

[8] A. Berthod, Chiral Recognition Mechanisms, Anal. Chem. 78 (2006) 2093

[9] W. Yanli, R. Yanfang, L. Jun, S. Shaomin, D. Chuan, Characterization of room temperature phosphorescence of propranolol and the chiral discrimination between R- and S-isomers, Analyst 136 (2011) 299

[10] E.V. Anslyn, J.F. Andersen, V.M. Lynch, Colorimetric Enantiodiscrimination of α-Amino Acids in Protic Media, J. Am. Chem. Soc. 127 (2005) 7986

[11] G. Absalan, Y. Alipour, Z. Rezaei, M. Akhond, Determination of enantiomer compositions of propranolol enantiomers by chiral ionic liquid as a chiral selector and the UV-assisted spectrophotometric method, Anal. Methods 4 (2012) 2283

[12] R. Xiong, C. Lu, W. Zhang, Z. Zhou, X. Zhang, Facile synthesis of tunable silver nanostructures for antibacterial application using cellulose nanocrystals, Carbohydr. Polym. 95 (2013) 214

[13] R. Guzel, Z. Ustundag, H. Eksi, S. Keskin, B. Taner, Z.G. Durgun, A.I. Turan, A.O Solak, Effect of Au and Au@Ag core-shell nanoparticles on the SERS of bridging organic molecules, J. Colloid Interface Sci. 351 (2010) 35

[14] A.H. Alshehri, M. Jakubowska, A. Młozniak, M. Horaczek, D. Rudka, C. Free, J.D. Carey, Enhanced Electrical Conductivity of Silver Nanoparticles for High Frequency Electronic Applications, ACS Appl. Mater. Interfaces. 4 (2012) 7007

[15] G. Yang, J. Xie, F. Hong, Z. Cao, X. Yang, Antimicrobial activity of silver nanoparticle impregnated bacterial cellulose membrane: Effect of fermentation carbon sources of bacterial cellulose, Carbohydr. Polym. 87 (2012) 839

[16] W. Zhao, H. Wang, X. Qin, X. Wang, Z. Zhao, Z. Miao, L. Chen, M. Shan,Y. Fang, Q. Chen, A novel nonenzymatic hydrogen peroxide sensor based on multi-wall carbon nanotube/silver nanoparticle nanohybrids modified gold electrode, Talanta 80 (2009) 1029

[17] J. Llorca, A. Casanovas, M. Domínguez, I. Casanova, I. Angurell, M. Seco, O. Rossell, Plasma-activated core-shell gold nanoparticle films with enhanced catalytic properties, J. Nanopart. Res. 10 (2008) 537

[18] N. G. Bastús, F. Merkoçi, J. Piella, V. Puntes, Synthesis of Highly Monodisperse Citrate-Stabilized Silver Nanoparticles of up to 200 nm: Kinetic Control and Catalytic Properties Chem. Mater., 2014, 26 (9), 2836

[19] P.Raveendran, J. Fu, S.L. Wallen, A simple and ''green'' method for the synthesis of Au, Ag, and Au–Ag alloy nanoparticles, Green Chem. 8 (2006) 34

[20] P .Raveendran, J. Fu, S.L. Wallen, Completely "Green" Synthesis and Stabilization of Metal Nanoparticles, J. Am. Chem. Soc. 125 (2003) 13940

[21] A. Campiglio, Determination of naproxen with chemiluminescence detection, Analyst. 123 (1998) 1571

[22] Y. Wei, S. Wang, J. Chao , C. Dong, S.H. Shuang, M.C. Paau, M.F. Choi, An Evidence for the Chiral Discrimination of Naproxen Enantiomers: A Combined Experimental and Theoretical Study, J. Phys. Chem. C. 115 (2011) 4033

[23] S. Tong, Y. Guan, J. Yan, B. Zheng, L. Zhao, , Enantiomeric separation of (R, S)-naproxen by recycling high speed counter-current chromatography with hydroxypropyl-β-cyclodextrin as chiral selector, J. Chromatogr. A. 1218 (2011) 5434

[24] C. Liu , B. Li, C. Xu. Colorimetric chiral discrimination and determination of enantiometric excess of D/L-tryptophan using silver nanoparticles. Microchimica Acta**.** 181 (2014) 1407.

[25] Hebeish A, El-Rafie M, El-Sheikh M, El-Naggar ME. Nanostructural features of silver nanoparticles powder synthesized through concurrent formation of the nanosized particles of both starch and silver. Journal of Nanoparticle Research. 13 (2013) 1.

[26] C.E. Dalgliesh, The optical resolution of aromatic amino-acids on paper chromatograms, J. Chem Soc. 756 (1952) 3940

[27] V.A. Davankov, The nature of chiral recognition: Is it a three-point interaction? Chirality, 9 (1997) 99

[28] J. Goto, N. Goto, T. Nambara, Sensitive derivatization reagents for the resolution of carboxylic acid enantiomers by high-performance liquid chromatography J. Chromatogr. A 239 (1982) 559

[29] M. Fillet, L. Fotsing , J. Bonnard, J. Crommen, Stereoselective determination of S-naproxen in tablets by capillary electrophoresis. J. Pharm. Biomed. Anal. 18 (1998) 799

[30] K. Zhang, N. Xue, Z. Yuan, L. Li, X. Shi, L. Cao, Y. Du, Separation of the two enantiomers of naproxcinod by chiral normal-phase liquid chromatography J. Chromatogr. Sci. 49 (2011) 272.

[31] N.H. Hashim, S.J. Khan, Enantioselective analysis of ibuprofen, ketoprofen and naproxen in wastewater and environmental water samples. J. Chromatogr. A. 1218 (2011) 4746.

Caption and legends for figures

Fig. 1. Absorbance spectra of Ag nanoparticles: Conditions: pH of 6.0 KHP buffer, ionic strength 0.01(M) and temperature 28 °C.

Fig. 2. The FT-IR spectra of starch and starch-AgNPs

Fig. 3. The TEM image of starch-AgNPs, inset AgNPs with a starch shell

Fig. 4. XRD pattern of the starch-AgNPs

Fig. 5. (A)- Absorbance spectra of NAP in methanol (1.4×10^{-2} M). (B)- Absorbance spectra of AgNPs with S-and R-NAP (concentration of enantiomers 1.4×10^{-4} M). Reaction conditions were pH of 6.0, ionic strength 0.01 M, temperature 28 °C, time 8 min.

Fig.6. Circular dichroism spectra of S-and R-NAP and starch-AgNPs

Fig. 7. a) Effect of pH, b) KHP concentration, c) volume of AgNPs, d) temperature, e) incubation time on chiral determination of 1.4×10^{-4} M of R-and S-NAP.

Fig. 8. Absorption spectra at various (A)-S-NAP and (B)-R-NAP concentration were monitored by UV-Vis spectroscopy under optimum conditions. Reaction conditions were pH of 6.0, temperature 28 °C, volume of Ag nanoparticles 200.0 μL, ionic strength 0.01 M, time 8 min.

Fig. 9. Calibration curve of naproxen enantiomers. Experimental conditions: pH of 6.0, temperature 28 °C, volume of Ag nanoparticles 200.0 μL, ionic strength 0.01 M, time 8.0 min.

**Fig. 10.** A typical simulated calibration curve for different mol ratio of S-NAP at 1.4×10^{-4} M (a-f: 0, 0.2, 0.4, .0.6, 0.8 and 1.0 respectively). Experimental conditions: pH of 6.0, temperature 28 °C, volume of Ag nanoparticles 200.0 μL, ionic strength 0.01 M, time 8.0 min.

Fig. 11. Calibration curve enantiomeric mixture of S-NAP (at 1.4×10^{-4} M). Experimental conditions: pH of 6.0, temperature 28 °C, volume of Ag nanoparticles 200.0 μL, ionic strength 0.01 M, time 8.0 min.
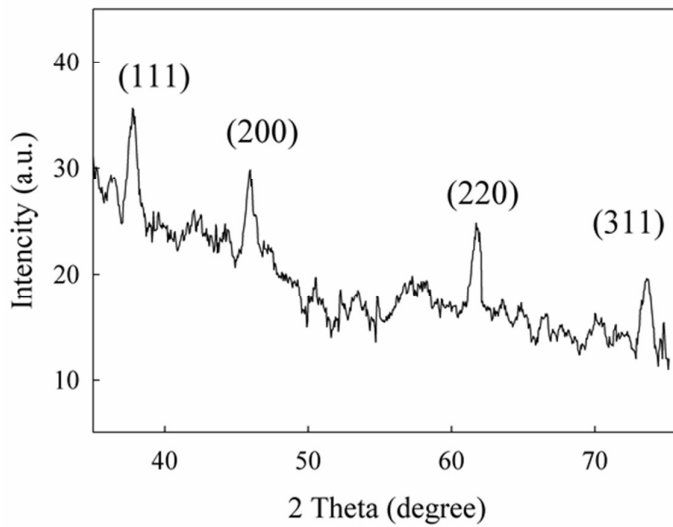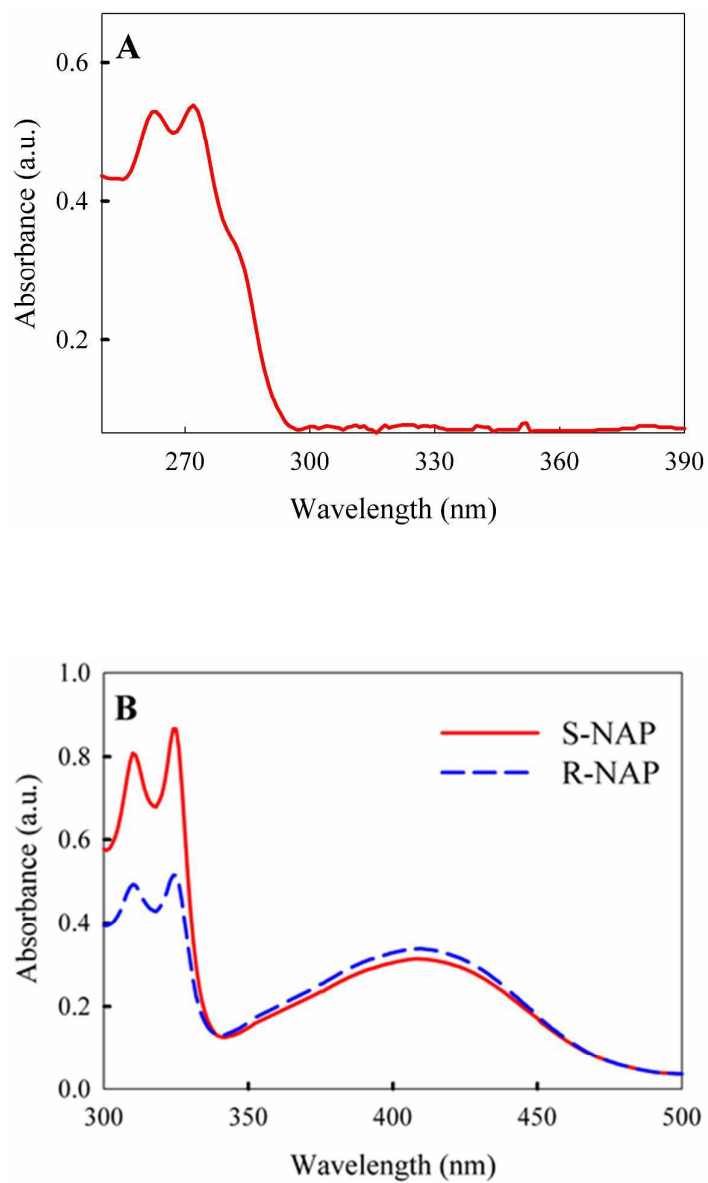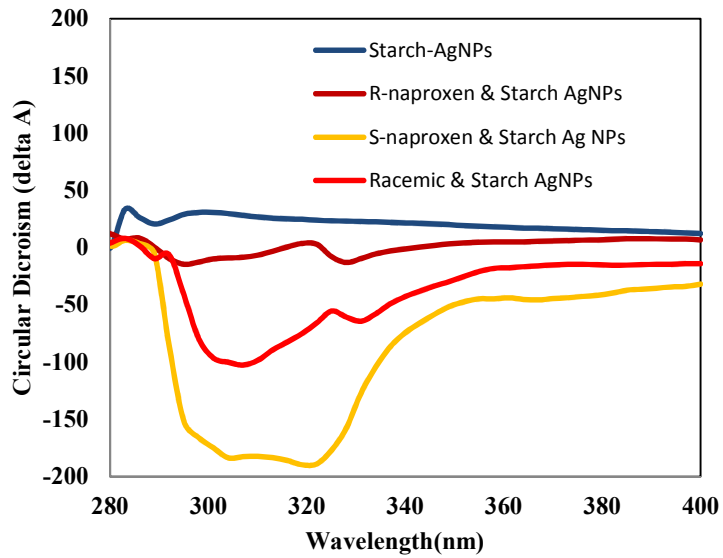
17
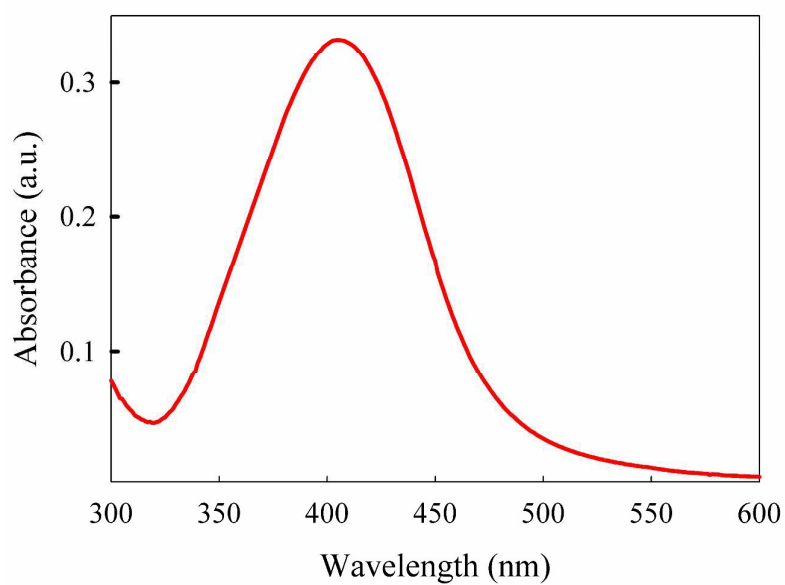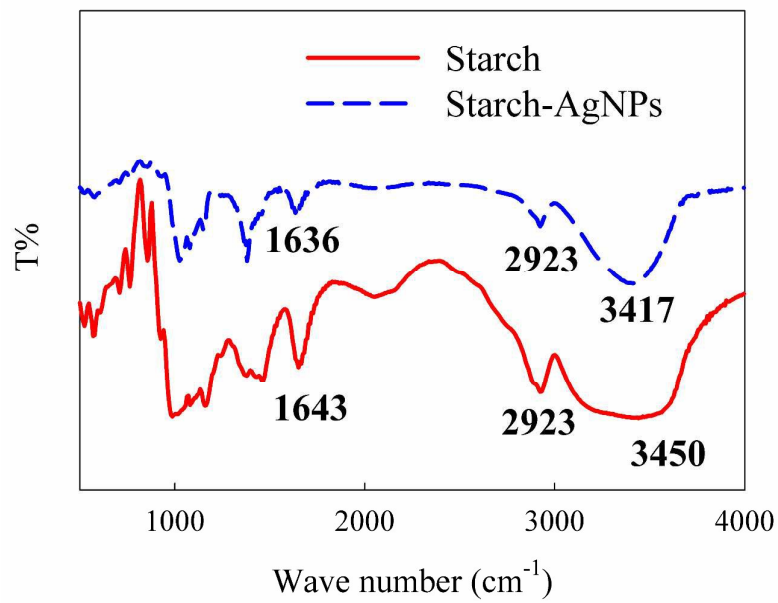
Fig. 1

Fig. 2
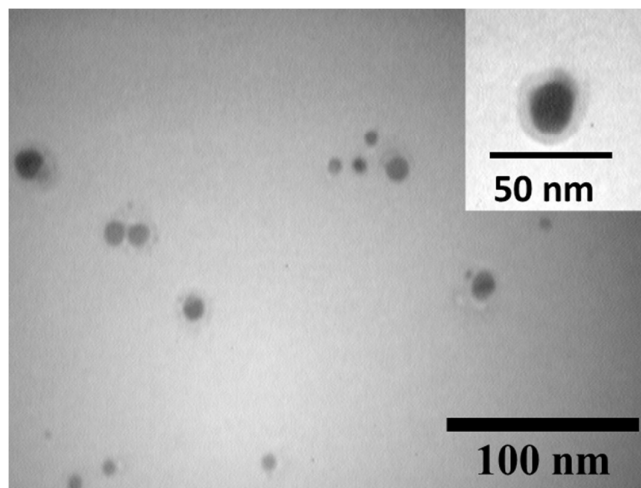
Fig. 3

1
2
3
4
5
6
7
8
9
10
11
12
13
14
15
16
17
18
19
20
21
22
23
24
25
26
27
28
29
30
31
32
33
34
35
36
37
38
39
40
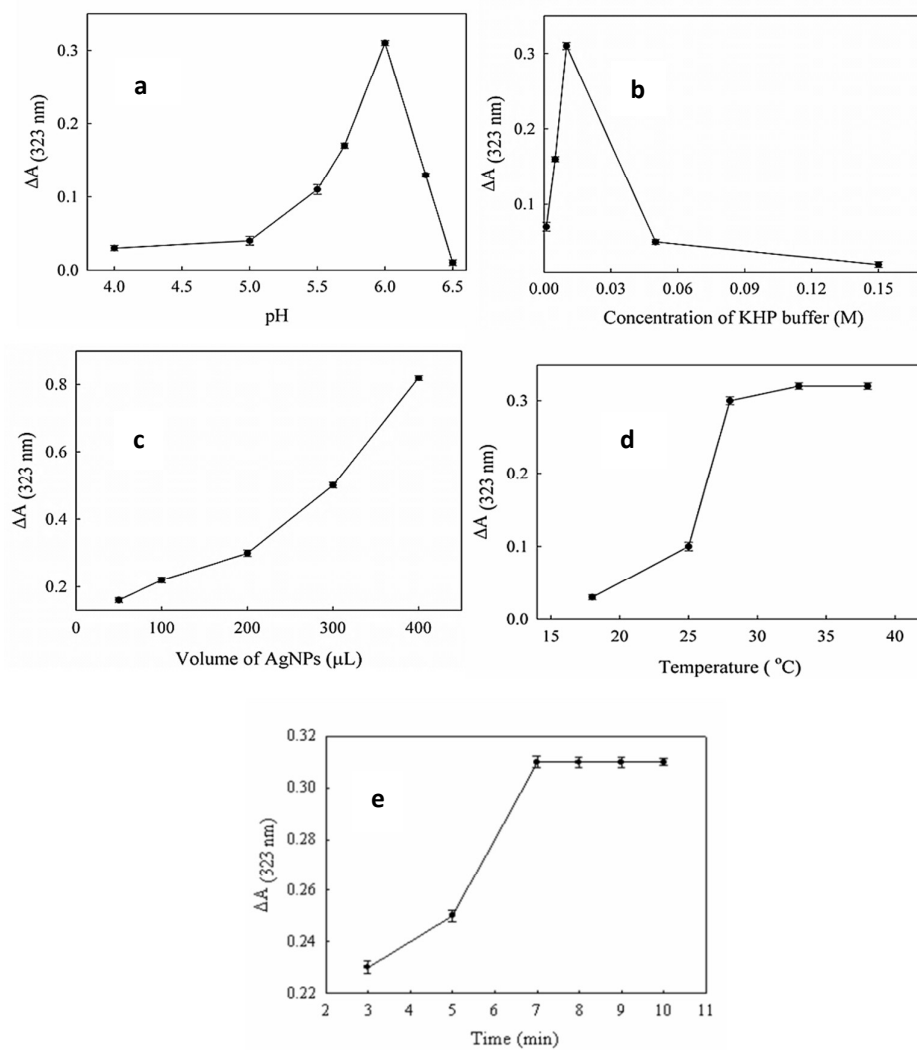41
42
43
44
45
46
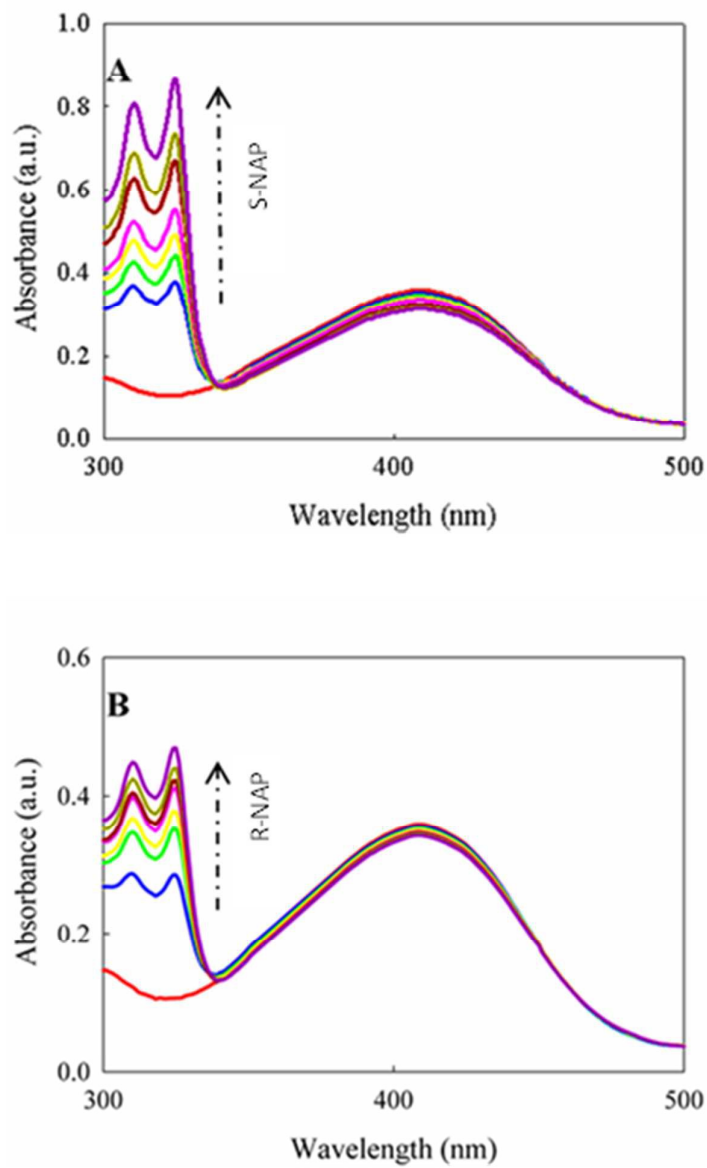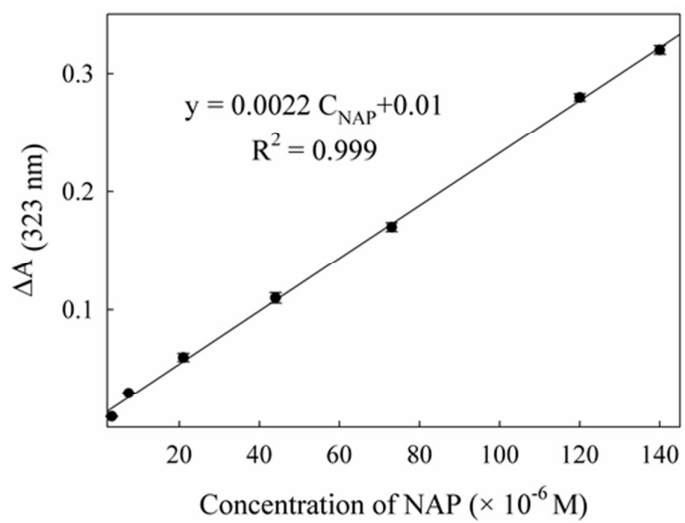47
48
49
50
51
52
53
54
55
56
57
58
59
60

Fig. 4

Fig. 5

Fig. 6

Fig. 7

Fig. 8

The graph shows ΔA (323 nm) on the y-axis and Concentration of NAP ($\times 10^{-6}$ M) on the x-axis, with the fitted equation:

$$y = 0.0022\ C_{NAP} + 0.01$$
$$R^2 = 0.999$$

Fig. 9

Fig. 10

$$y = 0.2972 \, x_{ee} + 0.4995$$

$$R^2 = 0.9993$$
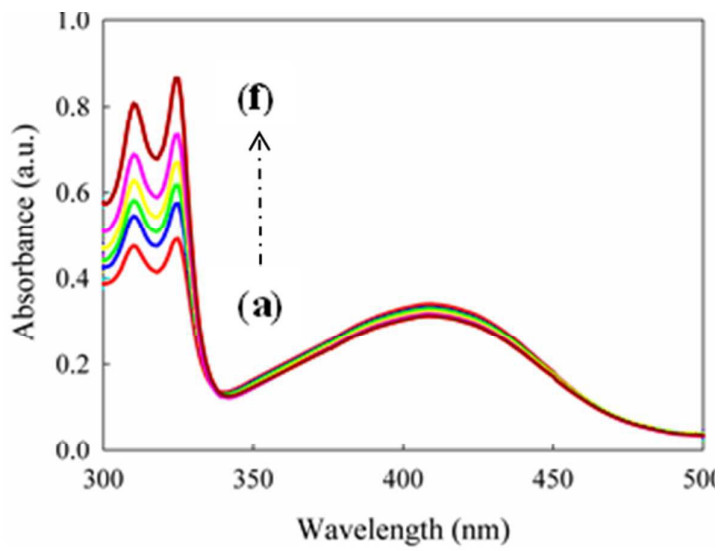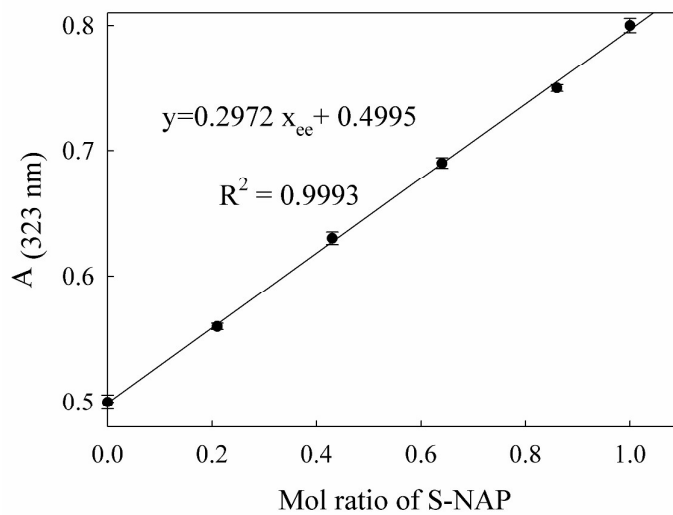
Fig. 11

Table 1: Determination of enantiomeric composition of S-Naproxen in synthetic samples

Experimental condition: pH of 6.0, $C_{Nap}=1.4\times10^{-4}$ mol L^{-1}, temperature 28 °C, time 7.0 min,

volume of Ag nanoparticles 200.0 µL.

Sample	Actual value (mole fraction)	Calculated value (mole fraction)	*%RE	% RSD
1	0.25	0.26	-4.0	1.2
2	0.5	0.47	-5.6	1.05
3	0.75	0.77	2.6	1.0

*Relative error = 100× (Experimental value − Actual value)/Actual value

Table 2: Comparison of figures of merit of the developed method with literature-reported methods.

Method	Linearity coefficient	*TEC(μM)	%RSD	%RE	Ref
HPLC	0.99	1.0	4.7	−	[28]
Capillary electrophoresis	0.9969	1.0	2.0	5.0	[29]
HPLC	0.999	86.8	1.0	-	[30]
Spectroscopy	0.9988	50.0	1.0	3.5	[11]
Gas chromatography	0.99	6.0	2.0	-	[31]
Spectroscopy	0.999	140.0	1.0	1.4	This method

*Total enantiomeric concentration=TEC